Proceedings of the ASME 2010 10th Biennial Conference on Engineering Systems Design and Analysis
ESDA2010
July 12-14, 2010, Istanbul, Turkey

ESDA2010-24614

OPTIMIZATION OF A HIGH PRESSURE SWIRL INJECTOR BY USING VOLUME-OF-FLUID (VOF) METHOD

Mohammad Rezaeimoghaddam*
Graduate student
Department of Mechanical Engineering
Ferdowsi University of Mashhad
Mashhad, Iran,
Email:m.rezaei.moghaddam@gmail.com

Hossein Moin
Graduate student
Department of Mechanical Engineering
Ferdowsi University of Mashhad
Mashhad, Iran,
Email:h.moin.jnr@gmail.com

M. R. Modarres Razavi
Professor
Department of Mechanical Engineering
Ferdowsi University of Mashhad
Mashhad, Iran
Email:m-razavi@um.ac.ir

Mohammad Pasandideh-Fard
Associate Professor
Department of Mechanical Engineering
Ferdowsi University of Mashhad
Mashhad, Iran
Email:mpfard@um.ac.ir

Rasool Elahi
Graduate student
Department of Mechanical Engineering
Ferdowsi University of Mashhad
Mashhad, Iran
Email:r.elahi.msc@gmail.com

ABSTRACT

In this paper, the effects of various geometric parameters of a high pressure swirl Gasoline Direct Injector (GDI) on the injection flow quality are investigated. The two-dimensional axisymmetric Navier-Stokes equations coupled with the Volume-of-Fluid (VOF) method were employed for simulation of the formation mechanism of the liquid film inside the swirl chamber and the orifice hole of the pressure swirl atomizer. To validate the model, results for base injector were compared in the steady state operation with those of available experiments in the literature. Good agreements were obtained for discharge coefficient (C_d) *and cone angle* (θ) *with experimental data. The effects of five characteristic geometric parameters of swirl injectors such as orifice ratio (orifice length to orifice diameter), angle of swirl chamber, orifice diameter, needle lift and needle head angle (assumed to be cone) were investigated. The results show that increasing the swirl chamber angle leads to an increase in mass flow rate and a decrease of the cone angle of liquid sheet. Through extensive simulations, geometric parameters of an optimum injector were obtained.*

*Corresponding Author

INTRODUCTION

In the recent years, many studies on swirl injectors have been carried out. However, most of the current knowledge is empirical. The GDI engine is one of the most favorable internal combustion engines due to low fuel consumption while maintaining low emissions. High pressure swirl injectors used in direct gasoline engines are critically important parts of GDI because their characteristics have a large effect on the performance. They are often used in GDI engines because they allow fine fuel spray at relatively low injection pressure. The swirl atomizers are made of several main parts; tangential slots, a swirl chamber, a needle and a discharge orifice. Figure 1 shows a schematic view of a high pressure swirl injector. During the injection process, pressurized liquid is forced to flow through tangential slots into the swirl chamber which results in developing a strong swirling motion of the liquid in the chamber. The flow is accelerated through the swirl chamber and then enters the orifice hole. The swirl motion of the liquid pushes it close to the wall and creates a zone of low pressure along the center line which results in back flow of air in the injector. The liquid emerges from the orifice as a conical sheet that spreads radially outwards due to centrifugal force. The conical liquid sheet becomes unstable and undergoes a complex process of breakup to form a spray of droplets. As it can be seen the geometry of high pressure swirl atomizer is fairly

simple but the flow through the atomizer is highly complex as it involves two phases, regions of recirculation, unsteady and turbulent flow. One important geometry parameter that relates to injector performance is injector constant. Injector constant is a dimensionless parameter first introduced by Doumas and Laster[1], it is the ratio of inlet area to the product of swirl chamber diameter and exit orifice diameter($K = A_p / D_s d_o$).

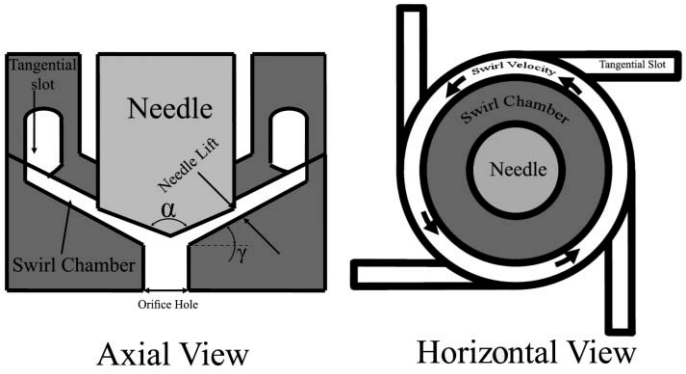

Figure1: SCHEMATIC VIEW OF A HIGH PRESSURE SWIRL INJECTOR.

The most important performance parameters are: mean spray droplet size (Sauter mean diameter), droplet size distribution, the spray cone angle, and the discharge coefficient. The mean drop size roughly correlates with the square root of the film thickness. It is known that the performance of the atomizer is governed by liquid properties, injection flow conditions and the atomizer geometry [2]. As the mass flow rate through the atomizer is increased from zero, the performance parameters change sharply at first, but eventually at high mass flow rate, the discharge coefficient, the film thickness, and the spray cone angle become steady to the variations in flow Reynolds number. This indicates that discharge coefficient, cone angle and air core radius do not depend on injection pressure and keep constant values [2]. Two important performance parameters in high pressure swirl injectors are calculated in steady state operation; the discharge coefficient and the cone angle. The discharge coefficient is the ratio of the actual to the maximum theoretical flow rate that is determined from the measured pressure drop across the atomizer.

$$C_d = \frac{\dot{M}_L}{\rho_L A_o \sqrt{2\Delta P/\rho_L}} \tag{1}$$

where $\dot{M}_L$, ρ_L, A_o and ΔP are the mass flow rate of injection liquid, the density of injection liquid, orifice area and the pressure drop across the injector respectively. The spray cone angle is calculated by:

$$\theta = 2\tan^{-1}\left(\frac{\overline{W_e}}{\overline{U_e}}\right) \tag{2}$$

where $\overline{W_e}$ and $\overline{U_e}$ are the average swirl and axial velocities at the orifice exit.

Due to the difficulties outlined earlier, the initial investigations of pressure swirl atomizers modeled the liquid as inviscid and the flow irrotational [3, 4]. Taylor [5] gave the most valid and pioneering theoretical treatment for potential flow in a swirl nozzle and predicted that the air core diameter and spray cone angle were inverse functions. Doumas and Laster [1] have reported an experimental study of such nozzles, measuring the discharge coefficient and the spray cone angle for more than 60 swirl atomizers covering a range of internal dimensions. They have developed zero dimensional models where fluids were assumed inviscid. Dumouchel et al [6] studied the two-dimensional viscous flow inside a pressure-swirl injector by numerically solving the streamfunction and vorticity equations. They have used the Bloor and Ingham [7] analysis for the boundary-layer flow above a flat disk and they estimated the proportion of the fluid that enters the orifice through the boundary layer. The first three-dimensional computational analysis on internal flow in the high pressure swirl injector was carried out by Ren et al [8]. This approach has been completed [9] and the needle movement inside the injector simulated in transient flows in high pressure swirl injectors by using the FIRE commercial code. More recent studies as those conducted by Arcoumanis et al [10, 11] take into account both fuel and air flow. Cousin et al [12, 13] investigated zero and one dimensional models in order to find an estimation that is not time consuming. Also particle image velocimetry (PIV) and laser doppler velocimetry (LDV) methods and high speed digital camera was used to measure the velocity field in the swirl chamber, the film thickness variation in the exit orifice, the spray angle, and the intact length of the film [14-16]. The two-dimensional no-Swirl computational analysis was carried out by Moon et al [17] with CFD-ACE+ commercial code in order to investigate an optimized injector. Kub et al [18] simulated the flow inside high pressure swirl injector with viscous model with Star-CD commercial code. In this study Fuel-injectors are widely used as important parts in direct gasoline engines because their characteristics have a large effect on the engine performance.

In this paper various geometry parameters are studied in order to obtain an optimized high pressure swirl injector. A transient two-dimensional axisymmetric Navier-Stokes numerical model based on Volume-of-Fluid (VOF) technique is employed for accounting the liquid-gas surface interaction. A modified VOF technique based on Youngs' PLIC (Piecewise Linear Interface Construction) algorithm [19] is employed to simulate the two-phase flow through the injector chamber. In this method, governing equations for mass conservation and momentum conservation are solved in the entire domain where the density and viscosity of the fluid are calculated as weighted average of the corresponding properties of the two phases based on the phase volume fraction in each cell. In addition to the mass and momentum conservation equations, an equation for the volume fraction of each phase is solved. When the volume fraction not equal to zero and one, a fluid interface is present within the computational cell. The formation mechanism of the liquid film was simulated inside the slots and the discharge hole of the pressure-swirl atomizer. The code is also extended with the k-epsilon model for including turbulence effect. The needle lift assumed to be constant for each simulation and the influence of transient upward motion on the flow field was also negligible. Simulations were performed for one commercial injector in 4.5Mpa Injection pressure with N-heptane as the injected liquid. Good agreement between numerical results and

those of the available experiments were obtained. By using the validated code the effect of five geometric parameters of swirl atomizers such as orifice ratio (orifice length to orifice diameter), angle of swirl chamber, orifice diameter, needle lift and needle head geometry (assumed to be cone) were investigated. In order to obtain an optimum geometry for a high pressure swirl injector, an investigation of different injector characteristic geometries are carried out on its performance based on studying between discharge coefficient and spray cone angle. The results show that increasing the swirl chamber angle leads to an increase in mass flow rate and a decrease of the cone angle of liquid sheet.

NOMENCLATURE

A_o	Orifice area
A_p	Total inlet slot area
D_p	Inlet port diameter
C_d	Discharge coefficient
α	Needle cone angle
γ	Swirl chamber angle
θ	Spray cone angle
K	Atomizer constant
D_s	Swirl chamber diameter
d_0	Orifice hole diameter
L_s	Swirl chamber length
l_o	Orifice length
P	Static pressure
Q	Volume flow rate
u	Axial velocity component
v	Radial velocity component
w	Swirl velocity component
ρ	Density
$\vec{u}$	Velocity vector
G_k	Turbulence kinetic energy due to velocity gradients
S	Mass transfer source or sink term
f^1	Volume fraction of phase 1

GOVERNING EQUATIONS

Numerical simulations of the unsteady two-phase flow field in high pressure swirl injector are governed by the continuity equation and Navier-Stokes equations. The continuity equation is given by:

$$\frac{\partial \rho}{\partial t} + \nabla(\rho \vec{u}) = 0 \tag{3}$$

Due to the full axisymmetric flow field through the injector chamber, swirl velocity inside the injector is assumed negligible and the momentum equation for two-dimensional flows written as follows:

$$\frac{\partial(\rho \vec{u})}{\partial t} + \nabla(\rho \vec{u}\vec{u}) = -\nabla p + \nabla\left[\mu\left(\nabla \vec{u} + \nabla \vec{u}^T\right)\right] + \rho \vec{g} + F_{vol} \tag{4}$$

In spite of the presence of the swirl chamber that creates a three-dimensional flow configuration, in this paper due to long time that required for three-dimensional simulation, the two-dimensional axisymmetric swirl model was used for compute flow through the injector. Due to important role of the swirl velocity in flow inside the injector the tangential momentum equation for two-dimensional swirling flows added to the momentum equations written as follow:

$$\frac{\partial}{\partial t}(\rho w) + \frac{1}{r}\frac{\partial}{\partial x}(r\rho u w) + \frac{1}{r}\frac{\partial}{\partial r}(r\rho v w) = \frac{1}{r}\frac{\partial}{\partial x}\left[r\mu\frac{\partial w}{\partial x}\right] + \frac{1}{r^2}\frac{\partial}{\partial r}\left[r^3\mu\frac{\partial}{\partial r}\left(\frac{w}{r}\right)\right] - \rho\frac{vw}{r} \tag{5}$$

where x the axial is coordinate, r is the radial coordinate, u is the axial velocity, v is the radial velocity, and w is the swirl velocity.

The phase change boundary is defined by Volume-of-Fluid (VOF) method where a scalar field is defined whose value is equal to zero in the gas phase and one in the liquid. When a cell is partially filled with liquid, f has a value between zero and one. The discontinuity in f is propagating through computational domain according to:

$$\frac{df}{dt} = \frac{\partial f}{\partial t} + \vec{V}.\vec{\nabla} f = S \tag{6}$$

where S is the appropriate mass transfer source or sink term. Due to neglecting the cavitation phenomenon in this study"S"is considered to be equal to zero. The $k-\varepsilon$ renormalization group (RNG) model was also used in order to calculate turbulence effect. The RNG-based $k-\varepsilon$ turbulence model is derived from the instantaneous Navier-Stokes equations, using a mathematical technique. Transport Equations for the RNG $k-\varepsilon$ Model are as follows:

$$\frac{\partial}{\partial t}(\rho k) + \frac{\partial}{\partial x_i}(\rho k u_i) = \frac{\partial}{\partial x_j}\left(\alpha_k \mu_{eff}\frac{\partial k}{\partial x_j}\right) + G_k + G_b - \rho\varepsilon - Y_M + S_k \tag{7}$$

$$\frac{\partial}{\partial t}(\rho \varepsilon) + \frac{\partial}{\partial x_i}(\rho \varepsilon u_i) = \frac{\partial}{\partial x_j}\left(\alpha_\varepsilon \mu_{eff}\frac{\partial \varepsilon}{\partial x_j}\right) + C_{1\varepsilon}\frac{\varepsilon}{k}\left(G_k + C_{3\varepsilon}G_b\right) - C_{2\varepsilon}\rho\frac{\varepsilon^2}{k} - R_\varepsilon + S_\varepsilon \tag{8}$$

where G_k represents the generation of turbulence kinetic energy due to the mean velocity gradients. The quantities α_k and α_ε are the inverse effective Prandtl numbers for k and ε, respectively. S_k and S_ε are source terms. The model constants

are $C_{1\varepsilon}$ and $C_{2\varepsilon}$ and they were assumed 1.42 and 1.68 respectively [20]. Using the RNG model causes to better handle low-Reynolds-number and near-wall flows .Turbulence, in general, is affected by swirl in the mean flow. The RNG model provides an option to account for the effects of swirl or rotation by modifying the turbulent viscosity appropriately.

NUMERICAL METHOD

In the numerical simulation the second order upwind scheme was employed to discretize the momentum equations and the momentum equations are solved implicitly. Also the ripple algorithm substitutes the flux correction equations into the discrete continuity equation to obtain a discrete equation for the pressure correction in the cell.

The Hirt-Nichols [21] and Young PLIC [19] methods are widely used for the advection of the volume of fraction in Eq. 5. Although the Hirt-Nichols has been used in most two-phase simulations, in this study the Young method which is more accurate is employed. To begin the advection using Eq. 5, an intermediate value of f is introduced as:

$$\tilde{f} = f^n - \delta t \vec{\nabla}.(\vec{V} f^n) \tag{9}$$

and "divergence correction" completes the scheme:

$$f^{n+1} = \tilde{f} + \delta t(\vec{\nabla}.\vec{V}) f^n + \delta t(S^n) \tag{10}$$

This scheme initiates the distribution of *f* for velocity and pressure calculations in each time step. Because a single set of equations is solved for both phases, mixture properties are used as:

$$\begin{aligned} \rho &= f\rho_l + (1-f)\rho_g \\ \mu &= f\mu_l + (1-f)\mu_g \end{aligned} \tag{11}$$

where subscripts l and g denote the liquid and gas, respectively.

To compare the computational results with experimental measurements, the assumption of axisymmetric domain requires determination of an equivalent ''annular" inlet slot instead of the finite number of slots present in the real atomizer. The width of the ''annular" slot as well as the radial and tangential velocities at the inlet are calculated by equating the angular momentum, total mass flow rate, and the kinetic energy of the liquid at the inlet ports with those in the experiments. The inlet boundary condition was applied to the top of the swirl chamber of injector. In order to specify the boundary conditions on the inlet the radial and swirl components of the velocity must be calculated from (Eq. 8).

$$W_{inlet} = \frac{Q}{A_p}.\frac{D_s - D_p}{D_s} \text{ and } V_{inlet} = \sqrt{\left(\frac{Q}{A_p}\right)^2 - W_{inlet}^2} \tag{12}$$

where $W_{inlet}, Q, D_s, D_p, V_{inlet}$ are mean tangential velocity at inlet, mass flow rate, diameter of swirl chamber, inlet port diameter (inlet port assume to be annular), mean radial velocity at inlet respectively.

VERIFICATION OF SOLUTION GRID INDEPENDENCE AND MODEL VALIDATION

It is essential to validate the code with grid independence computational domain. For this reason several number of grid nodes (5500, 11800 and 16000) were selected and mesh study was carried out. To ensure grid independence of results, the values of discharge coefficient and spray cone angle were compared in different grid numbers.

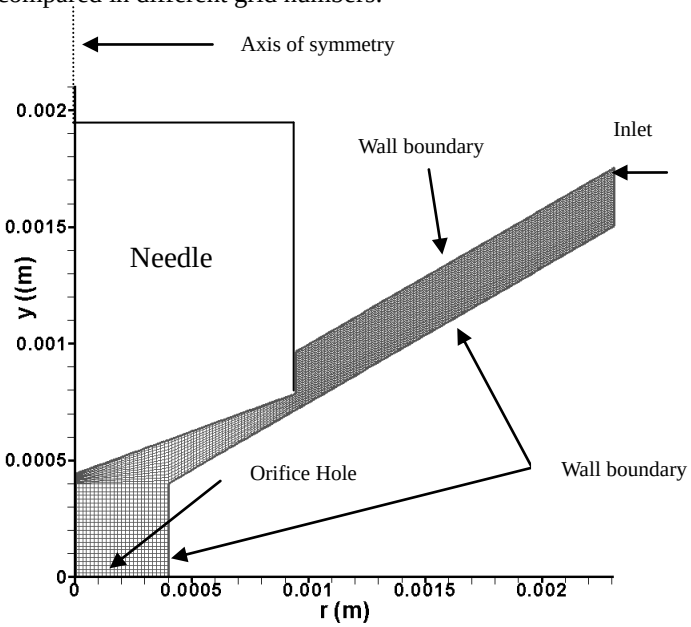

Figure 2: AXISYMMETRIC COMPUTATIONAL FINAL GRID USED FOR BASE INJECTOR.

With 11800 and 16000 cells, the discharge coefficient changed from 0.21095 to 0.212, and the spray angle remained unchanged at 87.99 The differences in the results using the two grids are very small and this indicates that 11800 cell grid is sufficient to get grid-independent results(see Fig. 2).

The N-heptane (C_7H_{16}) was the injected liquid with density of 684 kg/m^3, viscosity of 4.09×10^{-4} kg/m.s and surface tension of 0.02036 N/m. Calculations were carried out at 4.5MPa injection pressure and 300K constant temperature. The needle lift keeps constant values for all simulations. Liquid with uniform axial, radial and swirl velocity is assumed to enter in to the injector from the upper corner of swirl chamber.

Brief comparisons between numerical and those of available experiments for characteristic parameters of the injector such as discharge coefficient and spray angle have been shown in table 1 whereas the mass flow rate inside the injector obtained from the steady state operation. The numerical results shown that the differences between the VOF method prediction and experimental data were within -4.3% for discharge coefficient and +1.8% for spray cone angle respectively. The results show a good agreement between VOF simulation and the experimental data. This verification demonstrates VOF model is a reliable method.

Table 1: COMPARISION BETWEEN NUMERICAL AND EXPERIMENTAL DATA FOR A COMMERCIAL HIGH PRESSURE SWIRL INJECTOR

Method	C_d	error	θ(deg)	error
Current Study (VOF)	0.21	-4.3%	87.99	+1.8%
Experimental[17]	0.22	-	86.4	-

Figure 3 show the axisymmetric contours of volume of fraction and velocity magnitude inside the injector. Velocity magnitude has been suddenly changed when inter into the orifice hole and expels as a high velocity thin film with conical shape. The two-phase interface is also clearly predicts in velocity contour when high gradient of velocity magnitude between gas and liquid is calculated. The liquid domain is also demonstrates a detailed view of spread flow through the chamber. Effect of swirl chamber is precisely simulated as an accelerator developing strong swirling motion of the liquid.

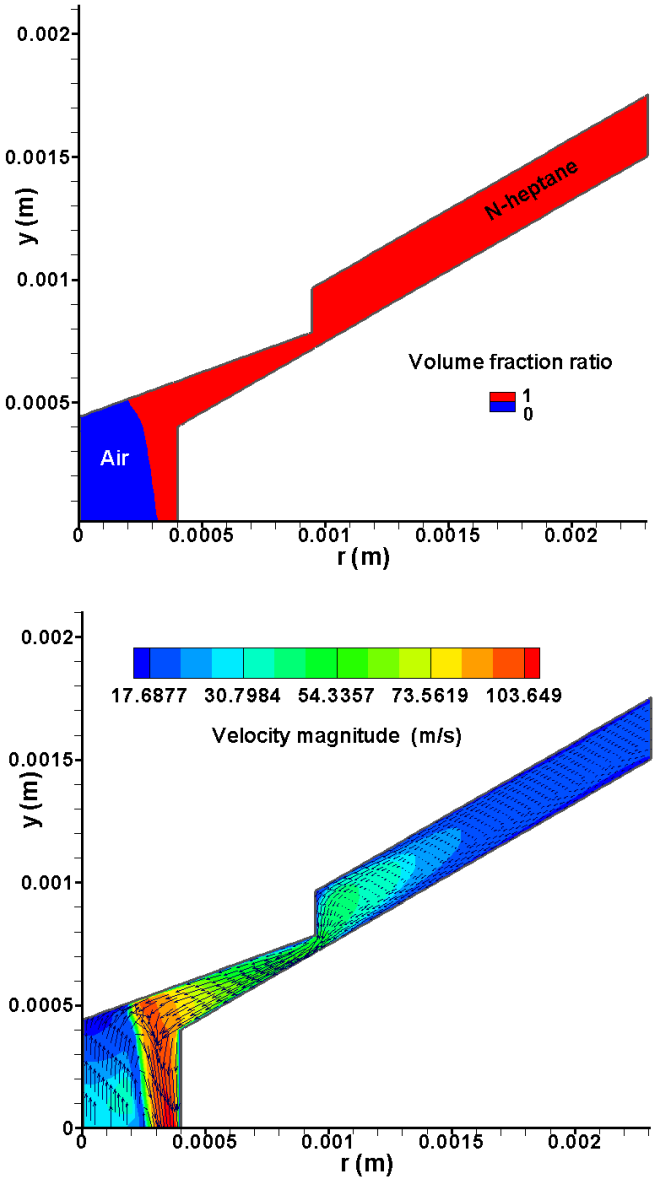

Figure 3: AXSYMITRIC CONTORS OF VOLUME OF FRACTION AND VELOCITY MAGNITUDE IN THE STEADY STATE OPERATION.

RESULTS AND DISCUSSION

In this section, we present an investigation of different injector characteristic geometries in order to improve its performance based on studying between discharge coefficient and spray cone angle. The effects of the length to diameter ratio of the orifice hole (lo/do), angle of swirl chamber, orifice diameter (d_o), needle lift and needle cone head angle on the performance of a simplex atomizer are numerically investigated. Two flow situations are important: constant mass flow rate through the injector and constant pressure drop across the injector. Here results are presented for both working conditions. Table 2 represents all spans of variations for characteristic geometry parameters which are considered in this study. The base geometric parameters are lo/do=1.0, d_o=0.8, needle cone angle = 140º, swirl chamber degree = 30º. While studying the effects of changes in lo/do, only lo is varied and all other dimensions are kept as base geometry. Similarly, lo is varied to change lo/do. For studying the effects of changes in swirl chamber angle and angle of needle cone the needle lift keep constant value as base injector. It is obvious that cases with different needle lift keep the base injector geometry too.

Table 2: VARIATION OF CHARACTRISTIC GEOMETRY PARAMETERS

Geometry parameters	lo/do	d_o (mm)	needle lift (μm)	needle cone angle
Range of variation	0.25 - 2	0.6 - 1	50 to 100	130º to 150º

EFFECT OF VARIATION IN LENGTH TO DIAMETER RATIO OF THE ORIFICE HOLE

Effect of variation in length to diameter ratio (lo/do) which is one of the main characteristic parameters in swirl injector performance has been considered. The values of lo/do are 0.25, 0.5, 1.0, 1.5 and 2.0 in this study. As it can be seen in the figure 4, a contour of velocity magnitude with velocity vectors in a closed view of swirl chamber and exit orifice has been shown. The interface between gas and liquid is clearly found in a very thin area which is the velocity magnitude has been changed rapidly and velocity vectors have opposite directions to each other. Due to comparison between a ratio with high discharge coefficient and high spray cone angle ($lo/do=0.25$) with a ratio with limited C_d and θ ($lo/do=1.0$), the results only are shown for these two different ratios of lo/do. The results show that the ratio of lo/do=0.25 creates a short orifice length and thereby it caused the swirled flow has higher spray cone angle. In contrast, long orifice lengths (lo/do=1and higher) have enough area to normalize the flow vectors and affect the spray cone angle. This phenomenon is due to effect of wall boundary that causes increasing the momentum of the flow and also the effect of

viscosity on the velocity profile. However, a very small orifice length seems favorable to achieve both higher C_d and θ, it is not applicable due to technical problems. For instance, enough length for a moderate swirl flow creation, unsteady operation of injectors and manufacturing limitations are most important reasons to have a minimum ratio of lo/do. Figure 5 shows that when lo/do is increased; the discharge coefficient is decreases significantly from 0.25 to 0.75.

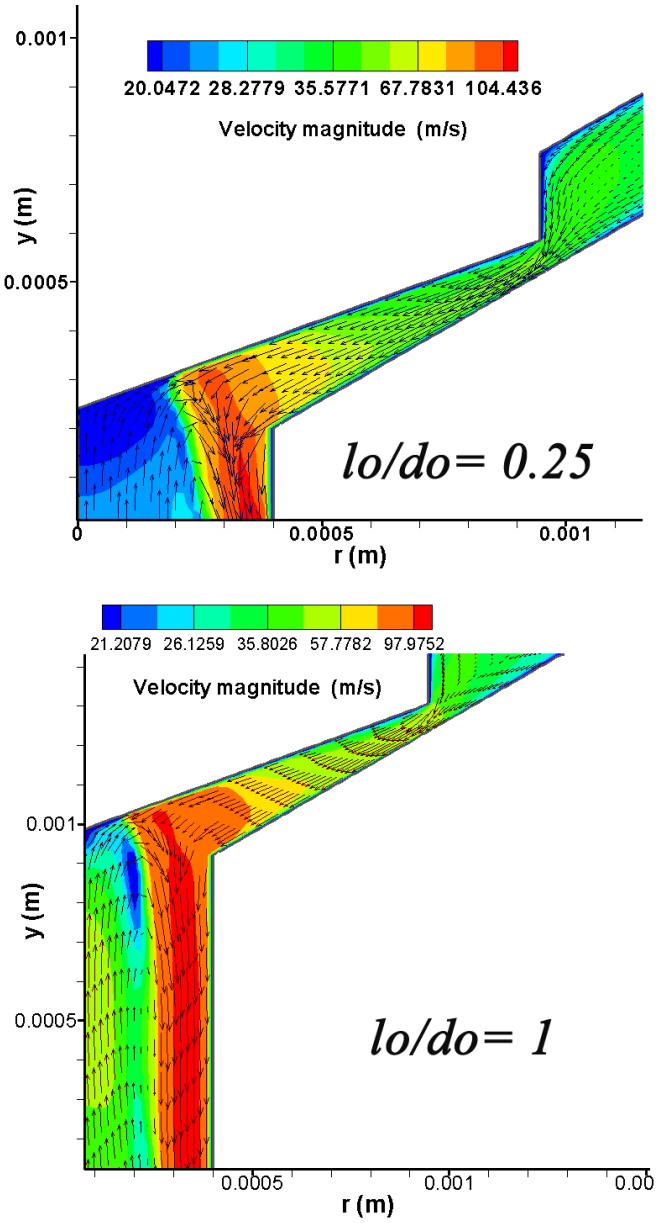

Figure 4: VELOCITY MAGNITUDE CONTOUR AND VELOCITY VECTOR IN TWO DIFFERENT ORIFICE LENGHT TO ORIFICE DIAMETER.

Larger value of lo/do corresponds to longer orifice length and results in an increasing decay of swirl energy. Figure 6 shows that as lo/do increases from 0.25 to 0.5, spray cone angle decreases dramatically; and as lo/do changes from 1 to 2, spray cone angle slightly decreases. Theoretically, this also results from increasingly decaying swirl energy at the exit for a longer orifice length. Figures 5 and 6 show that trend of discharge coefficient and spray cone angle are approximately the same. Thus the lo/do =0.5 is seems the best geometry of lo/do based on the base injector.

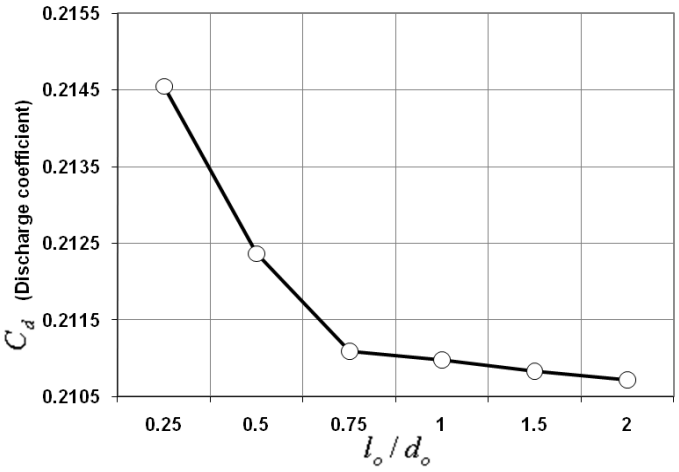

Figure 5: DISCHARGE COEFFICIENT VS. DIAMETER RATIO OF THE ORIFICE HOLE

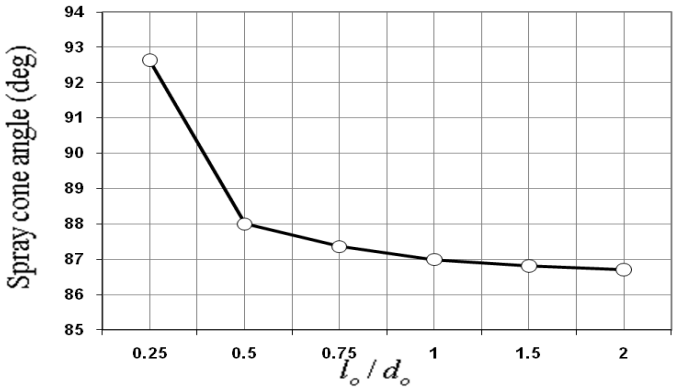

Figure 6: SPRAY CONE ANGLE VS. DIAMETER RATIO OF THE ORIFICE HOLE.

EFFECT OF VARIATION IN ORIFICE EXIT HOLE

The effect of orifice diameter is investigated to find its effect on the spray cone angle and discharge coefficient. Figure 7 shows a contour of velocity magnitude with velocity vectors in a closed view of swirl chamber and exit orifice for two different orifice diameter ($d_o = 0.6$ and $d_o = 1.0$). The images are shown a closed view of two mentioned injectors as minimum and maximum simulated orifice exit holes. With constant orifice length, increasing the diameter of orifice caused the volume of gas grows in the swirl chamber. On the other hand, swirled fluid affected by the vorticity of gas and changes its exit direction. Consequently, increasing the diameter of orifice causes a grater gas volume and creates stronger vorticity through the orifice hole. While the gas vorticity and swirled fluid has the same direction in the

interface, it assists to gain a bigger spray cone angle when the volume of gas comes more enough in the orifice hole area.

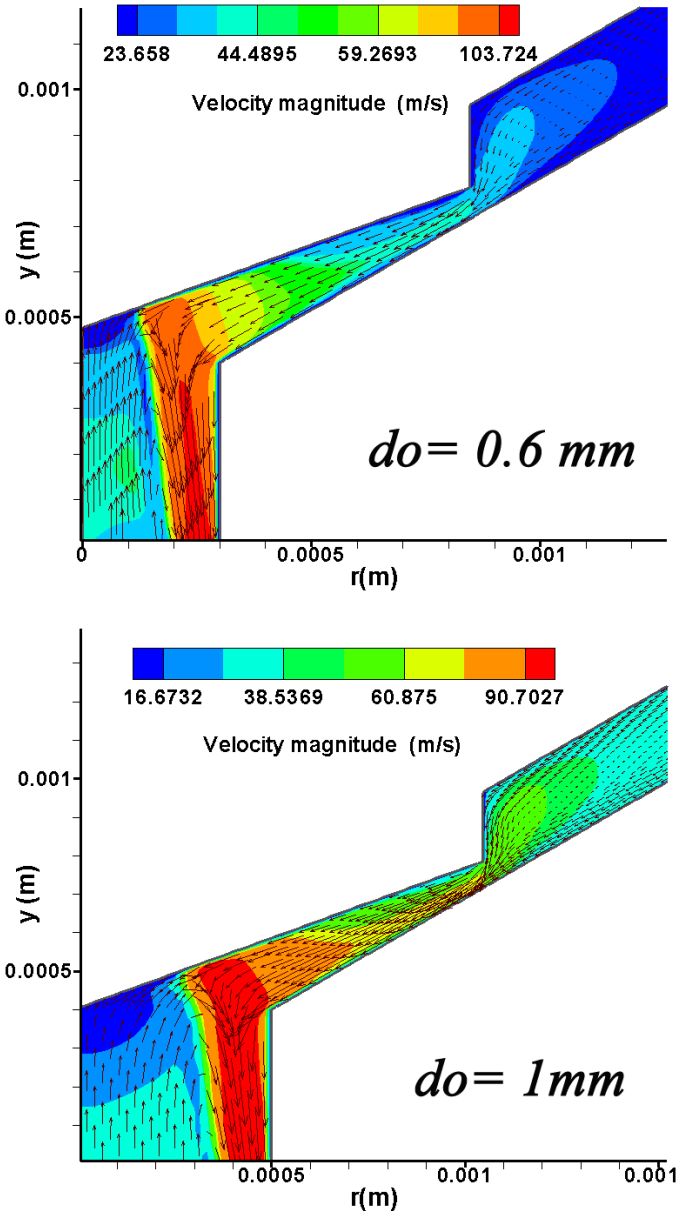

Figure 7: VELOCITY MAGNITUDE CONTOUR AND VELOCITY VECTOR IN ORRIFICE DIAMETER OF 0.6 AND 1.0 mm. (CLOSED VIEW)

Five values of d_o are considered 0.6, 0.7, 0.8, 0.9 and 1mm. Figure 8 shows the discharge coefficient variation with changing do. It can be seen that with increasing d_o from 0.6 to 1mm, discharge coefficient decreases from 0.275 to 0.17. The trend of do is linearly changed depend on C_d. Figure 9 illustrates the variation of cone angle with changing d_o. The behavior of cone spray angle is in the opposite of discharge coefficient while the orifice diameter changes. As it can be seen the amplitude of cone angle is between 78ºto 95º. The trend of do variation with spray cone angle is linear as well as the discharge coefficient. By comparison between the values of discharge coefficient and spray cone angle in different orifice the d_o =0.8 is obtained for the optimum orifice diameter.

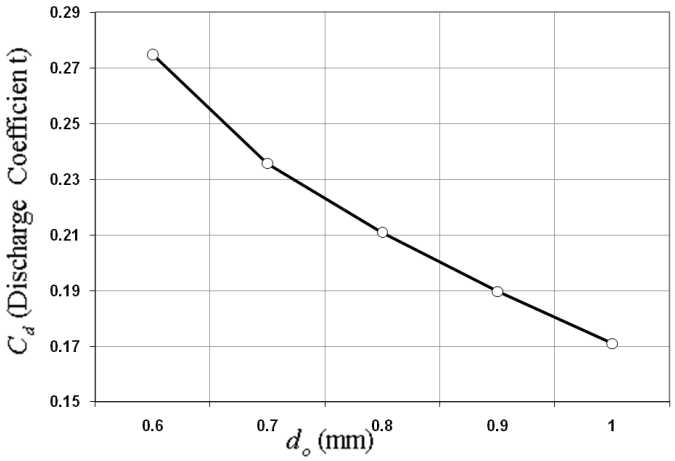

Figure 8: DISCHARGE COEFFICIENT VS. DIAMETER OF THE ORIFICE HOLE.

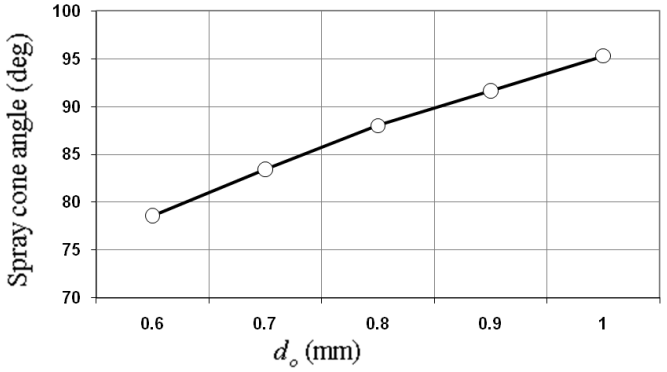

Figure 9: SPRAY CONE ANGLE VS. DIAMETER OF THE ORIFICE HOLE.

EFFECT OF VARIATION IN ANGLE OF SWIRL CHAMBER

The angle of swirl chamber and its effects on discharge coefficient and spray cone angle has been studied in this section. The needle cone angle is assumed to be constant through the simulations. The velocity magnitude contour and velocity vector are also shown in figure 10 for two different swirl chamber angles (35ºand50º). As it can be seen in this figure, when the swirl chamber angle increased, the volume of passage between needle and swirl chamber is also increased and a diverging zone could be create. While a part of this zone filled with the low momentum flow, the kinetic energy of expelled flow has been reduced. Thereby, the spray cone angle decreased. Moreover, growing the discharge coefficient is related to the increasing the angle of swirled chamber. Four values of swirl chamber angle are considered: 30 º, 35 º, 40 º and 45º. The variations of the discharge coefficient at the

orifice exit with changing swirl chamber convergence angle are shown in Fig. 11.

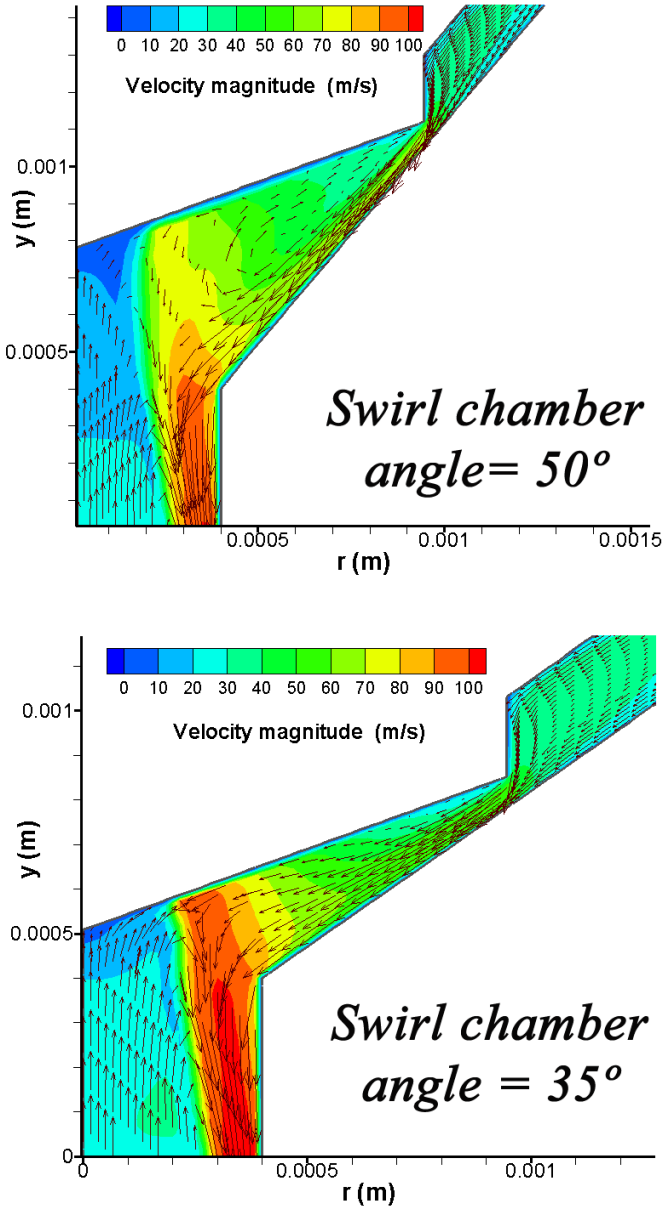

Figure10: VELOCITY MAGNITUDE CONTOUR AND VELOCITY VECTOR IN SWIRL CHAMBER ANGLE OF 35º AND 50º. (CLOSED VIEW)

The swirl chamber convergence angle has an opposite effect on performance parameters. With an increase in convergence angle, discharge coefficient increase and the spray cone angle decreases. The discharge coefficient variation with needle cone angle is given in Fig.11. As it can be seen the discharge coefficient increases slightly with increasing the angle of swirl chamber. The variation of spray cone angle with changing needle cone angle is shown in Fig.12. With increasing the swirl chamber angle from 30 º to 50º, the spray cone angle decreases by about 4.4%. In the figure 12, we can see that with increasing swirl chamber angle, decreases sharply from the values greater than 40º. Thus the optimum value for the swirl cone angle is considered 40 º.

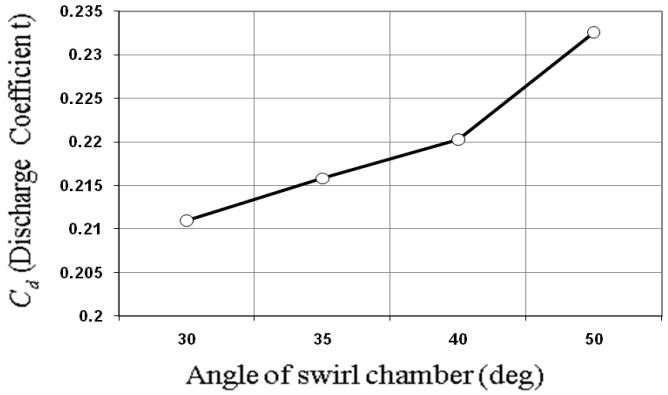

Figure 11: DISCHARGE COEFFICIENT VS. ANGLE OF SWIRL CHAMBER.

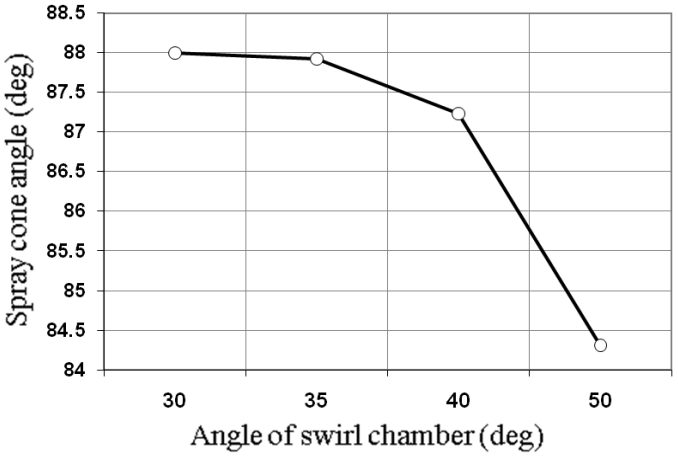

Figure 12: SPRAY CONE ANGLE VS. ANGLE OF SWIRL CHAMBER.

EFFECT OF VARIATION IN NEEDLE CONE ANGLE

The needle cone angle is other important geometric parameter which is considered for obtaining the optimum geometry in the high pressure swirl injector. The angle of swirl chamber is assumed to be constant in this study. Figure 13 shows a contour of velocity magnitude with velocity vectors in a closed view of swirl chamber and exit orifice for two different needle cone angle (130º and150º). When the passage between needle and swirl chamber is relatively parallel, the velocity profile inside this zone developed and viscous effect of the fluid flow become more important. Consequently, the total momentum of fluid has been reduced and spray cone angle gets smaller value. When the results of increasing the needle cone angle are studied, the effect of diverging passage as a boundary which is saves the momentum against the viscose shear stress is considerable. In addition, when the momentum saved the flow rate could persist against any looses and thereby the discharge coefficient has been grown.

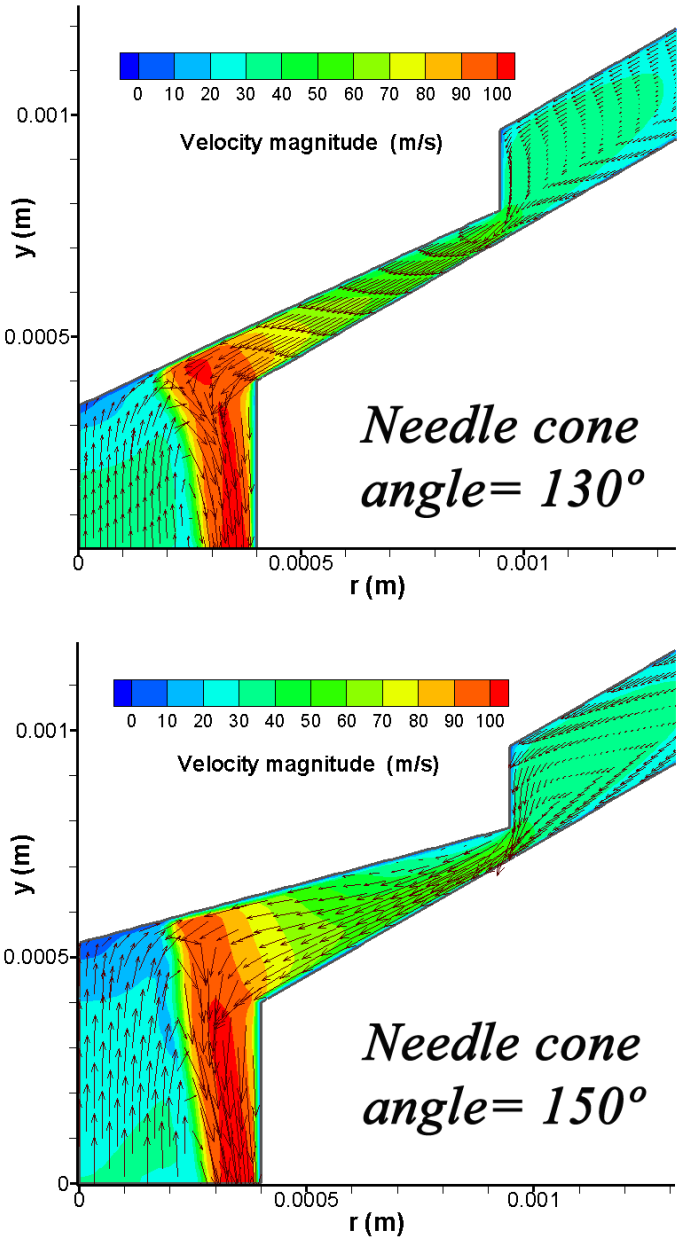

Figure 13: VELOCITY MAGNITUDE CONTOUR AND VELOCITY VECTOR IN NEEDLE CONE ANGLE OF 130º AND 150º. (CLOSED VIEW)

However, increasing the needle cone angle has limitations and the effective performances does not access from the distinct values. Four values of swirl chamber angle are considered (130º,135º,140 º,145 º and 150º). The variations in discharge coefficient and the spray angle are depicted in Figures 14 and 15 with varying needle cone angle. As it can be seen by increasing the needle cone angle the discharge coefficient increases suddenly. Figure 14 and 15 show that as needle cone angle increases from 130º to 140º, discharge coefficient and spray cone angle increases dramatically; and as needle cone angle changes from 140º to 150º discharge coefficient and spray cone angle slightly increases and approximately keep constant values. It is clear that the 140º is the optimum needle cone angle geometry for this type of injector.

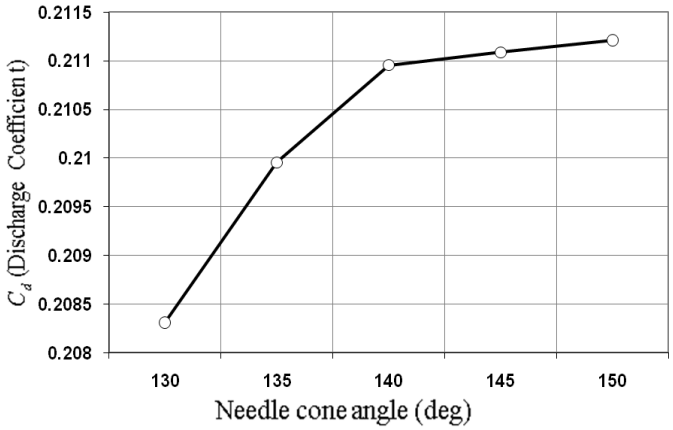

Figure 14: DISCHARGE COEFFICIENT VS. NEEDLE CONE ANGLE

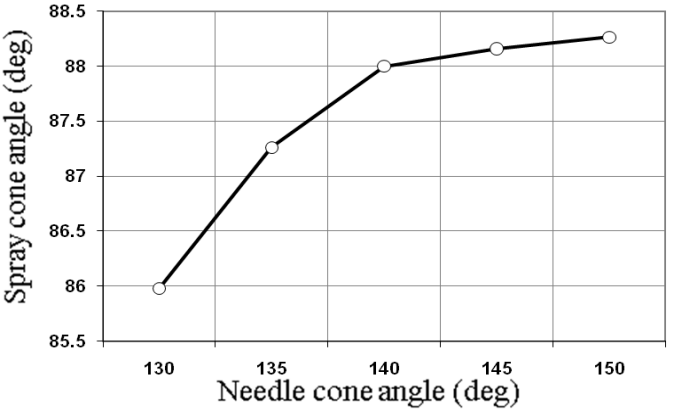

Figure 15: SPRAY CONE ANGLE VS. NEEDLE CONE ANGLE.

EFFECT OF VARIATION IN NEEDLE LIFT

Needle lift has been also simulated to finalize the numerical study on basic characteristic parameters of the swirl injector. As it can be seen in the figure 16, the velocity profile is completely sensitive to needle lift variation. While a flow with boundary layer has been created during the passage in lower lift, the effect of turbulence is negligible Seven values of needle lift are considered 50, 65, 70, 75, 80, 85 and 100µm. Figure 17 and 18 gives the variations of the discharge coefficient and spray cone angle at the exit with changing needle lift. As needle increases, discharge coefficient decreases and spray cone angle increases too.

Discharge coefficient increases with increasing needle lift in a linear trend. In addition spray cone angle increases as the same trend of discharge coefficient but in the opposite direction. With increasing the swirl chamber angle from 50µm to 100 µm, the spray discharge coefficient decreases from 0.212 to 0.208. The variation for spray cone is between 87.5º to 89º. Consequently due to these little differences for both discharge coefficient and spray cone angle and compromising between these values the optimum value for the needle lift is considered 75µm.

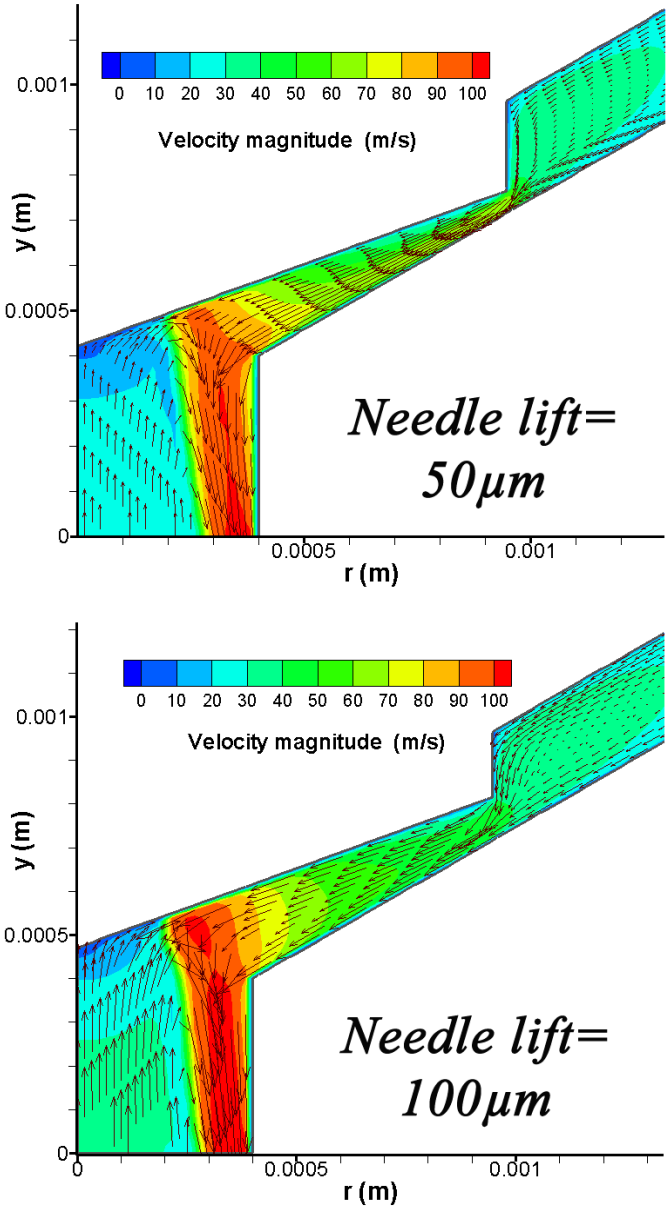

Figure 16: VELOCITY MAGNITUDE CONTOUR AND VELOCITY VECTOR IN NEEDLE LIFT OF 50 AND 100μm. (CLOSED VIEW)

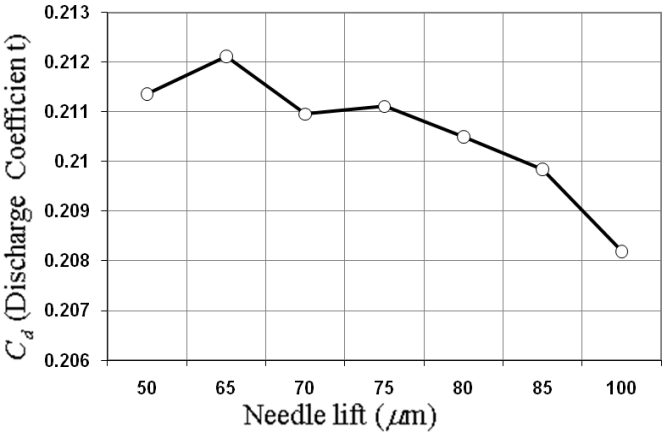

Figure 17: DISCHARGE COEFFICIENT VS. NEEDLE LIFT.

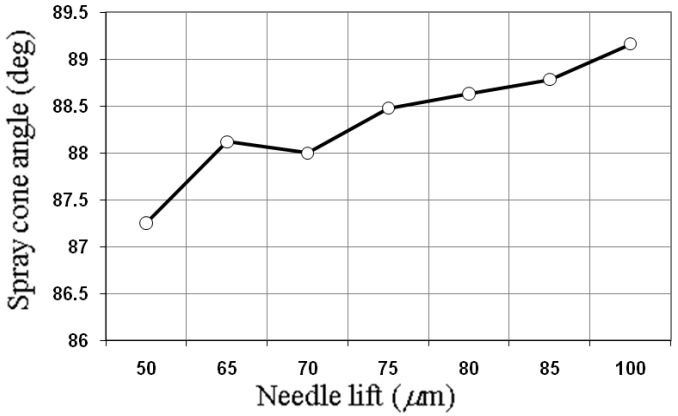

Figure 18: SPRAY CONE ANGLE VS. NEEDLE LIFT.

CONCLUSIONS

The optimization of the high pressure swirl injector is investigated by using 2D/axisymmetric Navier-Stokes equation. The Hirt-Nichols [20] and Young PLIC [19] methods are used for the advection of the volume of fraction in this study. To validate the model, results for base injector were compared in the steady state operation with those of available experiments in the literature. Good agreements were obtained for discharge coefficient (C_d) and cone angle (θ) with experimental data. Through the extensive numerical simulation the effects of changes in the ratio of length to diameter in orifice, increase in orifice diameter, swirl chamber angle, needle head cone angle and needle lift on the injector performance were studied. By compromising between discharge coefficient and spray cone angle which are the most important design parameters, the optimum geometry were calculated. The optimum values were obtained in constant pressure drop across the injector and constant inlet flow rate that enters to swirl chamber section. The ratio of length to diameter in orifice, the orifice diameter, swirl chamber angle, needle head cone angle and needle lift for an optimized injector were achieved 0.5, 0.8mm, 140º, 40ºand 75μm respectively.

REFERENCES

[1] Doumas, M., Laster, R. 1953,"Liquid-Film Properties for Centrifugal Spray Nozzles" *Chemical Engineering Progress*, pp.518-526.

[2] Lefebvre, A. H., 1989, Atomization and Spray, Hemisphere Publishing Co.

[3] Giffen, E., and Muraszew, A., "The Atomization of Liquid Fuels, John Wiley, 1953.

[4] Novikof, I. I.,1948 " Atomization of Liquids by Centrifugal Nozzles, *J. Tech. Phys.*, Vol. 18, no. 3, p. 345.

[5] Taylor, G.I., 1948, "The Mechanics of a Swirl Atomizer, in: Proceedings of the Seventh International Congress Applied Mechanics, vol. 2, no. 1, pp. 280.

[6] Dumouchel, C., Bloor, M., Dombrowski, N., Ingham, D. 1993,"Viscous Flow in a Swirl Atomizer" *Chemical Engineering Science*, vol. 48, no. 1, pp. 81- 87.

[7] Bloor, M. I. G. and Ingham, D. B., "Axially Symmetric Boundary Layer on a Finite Disk", Phys. Fluids, vol. 20, no. 8, p. 1228, 1977.

[8] Ren W. M., Shen J. , and Nally J. G. , 1997, "Geometric Effects Flow Characteristics of Gasoline High Pressure

Swirl Injector". *SAE Technical Paper No. 971641*, pp.1790-1797.

[9] Ren, W., Cousin, J., Nally, S., 1998,"Transient Flows in High Pressure Swirl Injectors" *SAE Technical Paper No. 980499*, pp.213-222

[10] Arcoumanis, C., Gavaises, M., 1999, "Modeling of Pressure Swirl Atomizers for GDI Engines", *SAE Technical paper*, pp. 516-532, Paper No 1999-01- 0500

[11] Arcoumanis, C., Gavaises, M., 2000, "Pressure Swirl Atomizers for DISI Engines: Further Modeling and Experiments", *SAE Technical paper*, pp.1225-1240 ,Paper No 2000-01-1044

[12] Cousin, J., Nuglisch, H., 2001,"Modeling of Internal Flow in High Pressure Swirl Injectors" *SAE Technical paper No 2001-01- 0963*, pp. 806-814

[13] Galpin, J., Cousin, J., Corbinelli, G., Sivieri, S., 2005, "A One Dimensional Model for Designing Pressure Swirl Atomizers" *SAE Technical paper No 2005-01-2101*.

[14] Hansen, K. G., Madsen, J., Trinh, C. M., Ibsen, C. H., Solberg, T. and Hjertager, B. H., 2002,"A computational and Experimental Study of the internal Flow In a scaled Pressure-swirl Atomizer" ILASS-Europe.

[15] Benjamin, M. , Mansour, A., Samant, U. G., Jha, S., Liao, Y., Harris, T. and Jeng, S. M., 1998, "Film Thickness, Droplet Size Measurements and Correlations for Large Pressure- Swirl Atomizers", American Society of Mechanical Engineers, Paper 98-Gt-537.

[16] Ma, Z., 2001,"Investigation on the Internal Flow Characteristics of Pressure-swirl Atomizer" Ph.D. Thesis, University Of Cincinnati, Department of Aerospace Engineering and Engineering Mechanics of the College of Engineering.

[17] Moon, S., Bae, S., Lee, C., 2001," Optimized Design of A New Gasoline Direct Swirl Injector" *Journal of Numerical Heat Transfer Part A*,pp.157-167

[18] Kubo, M., Sakakida, A., Liyama, A., 2001," Technique for Analyzing Swirl Injectors of Direct-Injection Gasoline Engines" *SAE Technical paper No 2001-01-0964*, pp.

[19] Youngs, D. L., 1982, "Time dependent multi material flow with large fluid distortion", *J. Num. Methods for Fluid Dynamics*, N.Y, 273-285.

[20] Lam, S., 1992,"On The RNG Theory of Turbulence" *Journal of Physics of Fluid*, A,4,pp. 1007-1017.

[21] Hirt, F. H. and Nichols, B. D., 1981, "A computational method for free surface hydrodynamics", *J. Comput. Phys.*, Vol. 39, p. 201

[22] Ibrahim, A., 2006, "Comprehensive Study of Internal Flow Field and Linear and Nonlinear Instability of an Annular Liquid Sheet Emanating from an Atomizer" PhD Thesis, Department of Aerospace Engineering and Engineering Mechanics of the College of Engineering.